General flowering in temperate forests arises from multi-timescale community synchrony

Valentin Journé[1], Jakub Szymkowiak[2], Jessie J. Foest[2], Marcin K. Dyderski[3], Szymon Jastrzębowski[4], Andrew Hacket-Pain[5], Michał Bogdziewicz*[2]

[1]Department of Biology, Faculty of Science, Kyushu University, Fukuoka, Japan

[2]Forest Biology Center, Institute of Environmental Biology, Faculty of Biology, Adam Mickiewicz University, Uniwersytetu Poznańskiego 6, 61-614 Poznan, Poland.

[3]Institute of Dendrology, Polish Academy of Sciences, Parkowa 5, Kórnik, 62-035, Poland.

[4]Department of Silviculture and Forest Tree Genetics, Forest Research Institute, Braci Leśnej 3, Sękocin Stary, 05-090, Raszyn, Poland.

[5]Department of Geography and Planning, School of Environmental Sciences, University of Liverpool, Liverpool, United Kingdom.

*corresponding author: michalbogdziewicz@gmail.com

keywords: Moran effect | mast seeding | spatial synchrony | seed production | community ecology | resource pulses | climate synchrony

Abstract

Community-wide "general flowering" has been regarded as a tropical phenomenon. Here, we show that temperate forests also exhibit community-wide flowering at the regional scale. Annual seed-production records for seven dominant tree species across 432 forest sites, analysed with timescale-explicit wavelet metrics, reveal landscape-scale synchrony structured by two periods — a 2–4-year band and a 5–8-year band — and associated with spatially coherent summer temperatures. This dual-band synchrony demonstrates that large-scale, cross-species reproductive alignment is an emergent property of temperate forest communities, implying shared climate cueing of reproduction and the potential for community-wide predator satiation. Since ~2005, the short- and long-period synchrony has weakened, and the short-period signal has shifted towards ~2 years (shorter period). Species-specific shifts in timescale structure no longer sum constructively, implying smaller, less predictable resource pulses at the community level, reduced community-wide predator satiation, and a decoupling of consumer–resource dynamics under continued warming.

Introduction

Spatial synchrony occurs when populations or ecological processes fluctuate in concert across different locations (1). Synchrony affects ecosystem stability when local dynamics combine to determine the regional response; synchronous fluctuations align and generate larger regional swings, whereas asynchrony dampens them (2). For example, when local populations rise and fall together, rescue effects are weakened because neighboring populations are likely to crash concurrently, elevating extinction risk (3). Synchrony also amplifies variability in regional crop yield when farm-level yields fluctuate in concert, while asynchrony across farms increases agrosystem resilience (4). Another striking example is the general flowering in tropical Asian forests, where hundreds of species, especially those of the Dipterocarpaceae family, flower synchronously at irregular multi-year intervals (2–10 years), creating resource pulses that reorganize seed predation, tree recruitment, consumer dynamics, and nutrient fluxes (5). These spectacular community-wide fluctuations have been viewed as unique to Southeast Asian dipterocarp

systems (5; 6). Here, we show that temperate forests also exhibit community-level synchronous fluctuations in seed production, revealed when dynamics are resolved by timescale.

Mass flowering or masting — the highly interannually variable seed production synchronized among conspecifics — is widespread in perennial plants (7; 8). Proximally, masting arises from processes operating on distinct timescales. At shorter interannual scales (~2–4 years), weather variation (called weather cues) shapes floral induction, pollination, and seed maturation (9). For example, hot summers can promote massive floral initiation for the following year (10; 11), and dry springs can enhance cross-pollination (12; 13). As reproduction responds to weather, shared weather patterns produce regional synchrony (14; 15). At lower frequency (~5–10 years), climate modes (e.g., North Atlantic Oscillation NAO or El Niño / Southern Oscillation ENSO) may align favorable conditions across flower-to-fruit maturation stages and over large areas, yielding sustained periods of elevated or depressed seed output (16; 17). For example, sequences of positive winter NAO, summer heat, and dry springs have aligned resource priming, bud initiation, and pollination, producing sustained periods of elevated seed production and continent-scale beech (*Fagus sylvatica*) mast years in Europe (17). Conversely, prolonged negative NAO has been associated with extended intervals of poor seed productivity (17). Because these processes operate on distinct timescales, community seed production likely contains multiple high- (~2–4 y) and low-frequency (~5–10 y) components that differ among species and sites in strength (variance share) and phase (peak timing) (16; 18; 17). Analysing the synchrony of reproduction across all timescales simultaneously mixes these components; fluctuations at different frequencies can cancel and make community synchrony appear weak or absent (2; 1).

Co-occurring species in the same region often respond to similar weather cues, likely reflecting shared selective pressures or benefits of intraspecific masting synchrony, rather than phylogenetic history (19). In temperate European trees, interannual variation in seed production is linked to spring and summer temperature cues (11; 20), while at lower frequencies many species show coherence with the NAO (17). Within species, regional synchrony is high and extends over hundreds of kilometers (14; 21). By contrast, regional among-species synchrony remains largely untested. Within-site studies often detect significant covariation among species

(22; 23), but one of the few regional analyses reported low or absent community-wide synchrony (21). However, those inferences relied on period-pooled metrics that conflate high- and low-frequency components and cannot resolve timescale structure, motivating a timescale-explicit analysis here.

Progress on community-wide synchrony in seed production was limited by two constraints: data and methods. Seed production records were often short and local (24). Crucially, multi-species records spanning large areas and decades were unavailable, making multi-year structure at regional scales difficult to detect. Yet, while no single site or species may exhibit a clear "community–mass flowering" signal on its own, shared high- or low-frequency modes can align across sites and sum to large regional pulses (2; 1). Standard tools for analyzing synchrony (e.g., correlations, regressions) pool across periods and cannot separate short- from long-timescale fluctuations or attribute their causes, especially when effects interacted or were phase-shifted across space (1). Timescale-specific wavelet approaches now address these gaps: they quantify synchrony by time and period, identify timescale-specific links to candidate drivers and their lags, and partition how much synchrony is explained by individual drivers versus their interactions (25; 26; 1). We build on this framework to test for community-level synchrony in temperate forests, revealing how high- and low-frequency components combine to produce regional pulses.

Recent evidence shows that synchrony of ecological phenomena, such as insect abundance or tree growth (25; 27; 28), is changing under climate warming. Increased synchrony is emerging as an important consequence of climate change (28), often reflecting increased spatial coherence in weather patterns (28; 1). However, reproductive synchrony in masting species may respond differently (8). Because masting depends not only on shared weather cues but also on a plant's internal resource dynamics (9; 29), increasing climatic synchrony does not necessarily translate into greater reproductive synchrony (30). In fact, the opposite is expected: when warming increases weather cue frequency (e.g., warm summers), repeated triggering of reproduction depletes plant reserves and weakens the weather cue–masting coupling (31; 29). This mechanism should first shorten effective cycle length (18) and can then reduce or cancel synchrony even under increasingly coherent weather (31; 30) - producing a decoupling of biological coherence from climatic coherence. If such declines in regional synchrony extend across co-flowering

species, the multi-year windows of seed abundance and scarcity that once organized consumer dynamics can fragment into smaller, out-of-phase events, dulling trophic pulses, and reshaping nutrient and consumer cascades at landscape scales.

Here, we used annual seed-production records for seven dominant, forest-forming tree species across 431 sites in temperate Europe (Poland), collected between 1987 and 2022, to test for community-wide synchronous reproduction, its timescale-specific drivers, and temporal trends. We formulated three predictions. First, because reproduction in temperate trees is driven by largely shared summer and spring temperature cues at interannual scales (20; 19) and because resource–cue coupling generates a dominant 2–4-year period (32; 29), community-level synchrony should emerge at short periods. Second, species such as European beech and spruce (*Picea abies*) share low-frequency coherence with the NAO, so a secondary 6–12-year mode should co-occur across species (17). Third, rising summer temperatures should increase cue frequency, shorten effective masting periods, and — over time — decrease masting synchrony (18; 31; 30).

Results

Table 1: Relationship between masting synchrony and driver variables. P-values are from tests of spatial wavelet coherence. We constructed separate models for weather variables and NAO indices. Phase relationships (ϕ) for drivers were obtained from multi-predictor wavelet linear models. Phase relationships are given in fractions of π, for significant drivers. Negative phase relationships that are not approximately in-phase ($\phi \approx 0$, interpreted as $-0.25 < \phi < 0.25$) or anti-phase ($\phi \approx \pm 1$, interpreted as $\phi < -0.75$ or $\phi > 0.75$) indicate that masting lags the driver variable; positive phase relationships that are not approximately in-phase or anti-phase indicate that mast peaks precede those of the driver variable. Cross term is diagnostic of the wavelet Moran theorem; no values were reported for NAO indices because those climate indices are not spatially resolved. Species-specific drivers are reported in Table S1.

Driver variable	Timescale	p-value	Mean phase (ϕ)	Cross terms
ΔT	2-4	0.01	-0.34	3.18
	5-8	0.003	-0.62	30.2
T_{spring}	2-4	0.79	-	3.18
	5-8	0.93	-	30.2
NAO_{winter}	5-8	0.12	-	-
$NAO_{summmer}$	5-8	0.48	-	-

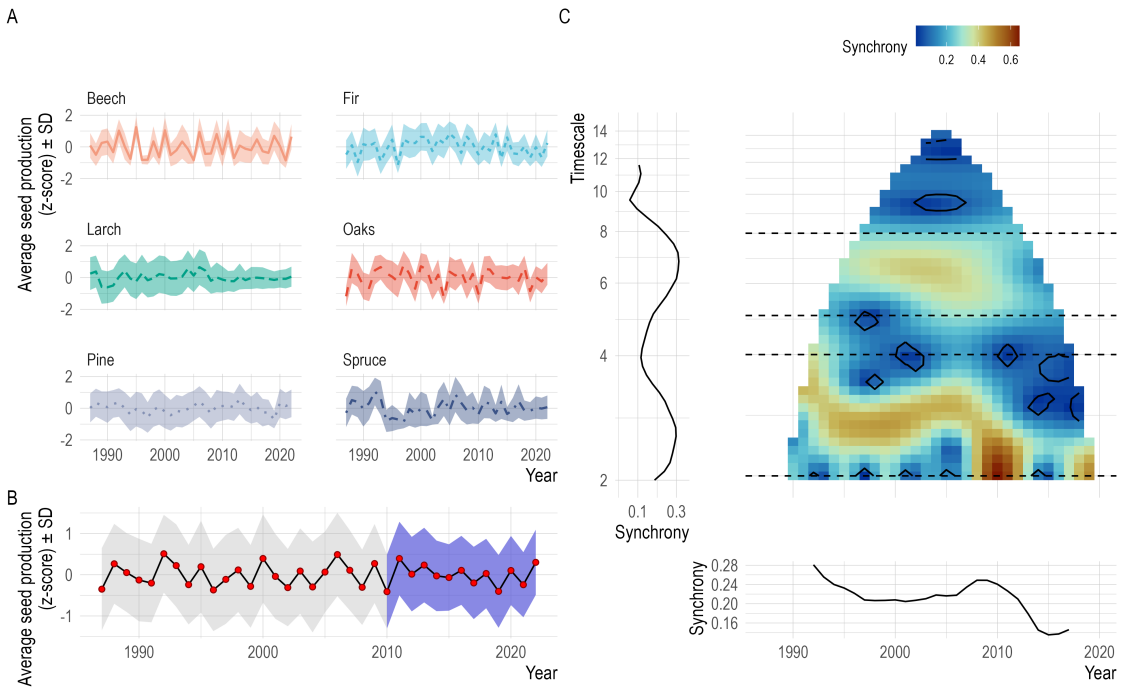

Figure 1: Dual-band synchrony organizes community-wide masting in temperate forests. A) The interannual variation in seed output in the studied taxa; the time series are summarised at the species level. Before analysis, series were normalised and detrended (see Methods). Each line shows annual means across all sites for each species (±SD). B) Region-wide synchrony cycles emerge through among-species synchrony. Post 2010, such synchrony declined strongly, dampening the pre-existing phase of 2-4 years (highlighted in purple). The black line shows annual means across all sites and species (±SD). C) Wavelet mean field (WMF) magnitude plots of time- and timescale-specific spatial synchrony in seed production for all studied species. Black contours indicate statistically significant synchrony (using standard significance level, $p < 0.05$) as determined from the wavelet phasor mean field (WPMF), with the WPMF plots in Fig. S1. Side panels are averages across times (bottom) or timescales (left side). In this analysis, time series from all species were analysed jointly and therefore reflect the combined effects of within- and among-species synchrony, i.e., community-level synchrony. Species-specific (within-species) synchrony is shown in Fig. 2. The vertical dashed lines highlight the synchrony bands analyzed with spatial wavelet coherence. The analysis is based on seed production data collected between 1987 and 2022 across 432 sites Poland (Fig. 4) for seven tree species: silver fir (*Abies alba*), European beech (*Fagus sylvatica*), European larch (*Larix decidua*), Norway spruce (*Picea abies*), Scots pine (*Pinus sylvestris*), sessile oak (*Quercus petraea*), and pedunculate oak (*Quercus robur*). Before 2008, oak harvests were not distinguished by species; therefore, records for the two oaks were pooled for the entire time series (see Methods). Results based on an independent dataset replicated the patterns - both the dual-band synchrony and its temporal decline - and are provided in Fig. S2.

Dual-band synchrony organizes community-wide masting (2–4 and 5–8 years). Across seven dominant tree species, community seed production was synchronized at two distinct periods: a short-period 2–4-year band and a long-period 5–8-year band (Fig. 1). Both the Wavelet Phasor Mean Field (WPMF) (Fig. S1) and the Wavelet Mean Field (WMF) showed this dual-band structure, indicating alignment in phase (timing; WPMF) as well as in phase and amplitude (WMF) across species and sites, yielding region-wide seed pulses. Critically, the same two-band structure was replicated in a second independently collected dataset comprising 16 regional seed production records spanning 32 years for the same species set, confirming

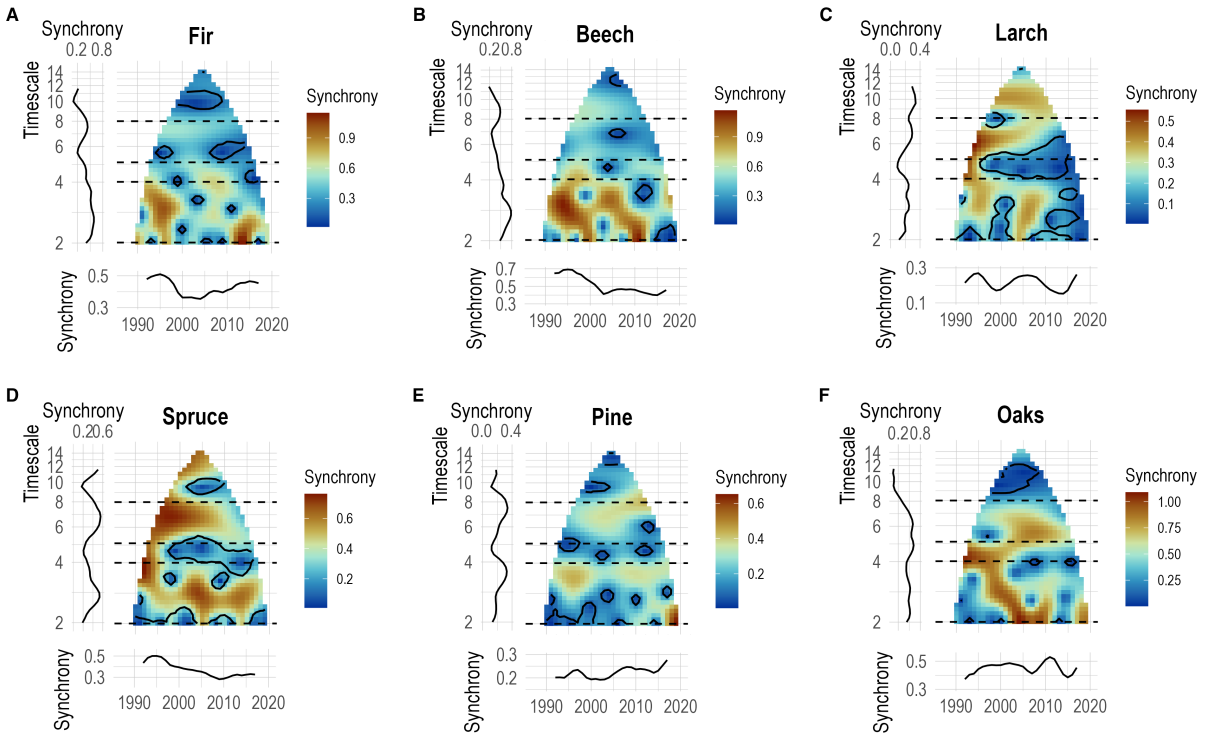

Figure 2: Dual-band intraspecific synchrony that underlies community-wide masting in temperate forests. Wavelet mean field (WMF) magnitude plots of time- and timescale-specific spatial synchrony in seed production for each species separately. Black contours indicate statistically significant synchrony as determined from the wavelet phasor mean field (WPMF), with the WPMF plots in Fig. S1. Side panels are averages across times (bottom) or timescales (left side). The vertical dashed lines highlight the synchrony bands analyzed with spatial wavelet coherence. The analysis is based on seed production data collected between 1987 and 2022 across 432 sites in Poland (Fig. 4). Species include silver fir (*Abies alba*), European beech (*Fagus sylvatica*), European larch (*Larix decidua*), Norway spruce (*Picea abies*), Scots pine (*Pinus sylvestris*), sessile oak (*Quercus petraea*), and pedunculate oak (*Quercus robur*). Before 2008, oak harvests were not distinguished by species; therefore, records for the two oaks were pooled for the entire time series. Results based on an independent dataset replicating the patterns are provided in Fig. S3.

that the community-wide mass-reproduction signal is robust to sampling design and data source (Fig. S2).

The community-wide synchronous reproduction arises from a shared timescale structure of synchrony within species. Within the studied species, WMF shows regional phase synchrony at a period of 2–4 years and secondary coherence at 6–10 years (Fig. 2). The synchrony estimated with the WPMF (Fig. S1) generally matched one estimated with WMF (Fig. 1), indicating both phase alignment and uniform amplitude: sites share years of peak and failed reproduction, as well as the magnitude of those events. The similar phase and amplitude synchrony, when summed across species, appears to drive the region-scale pulses in community-wide reproduction.

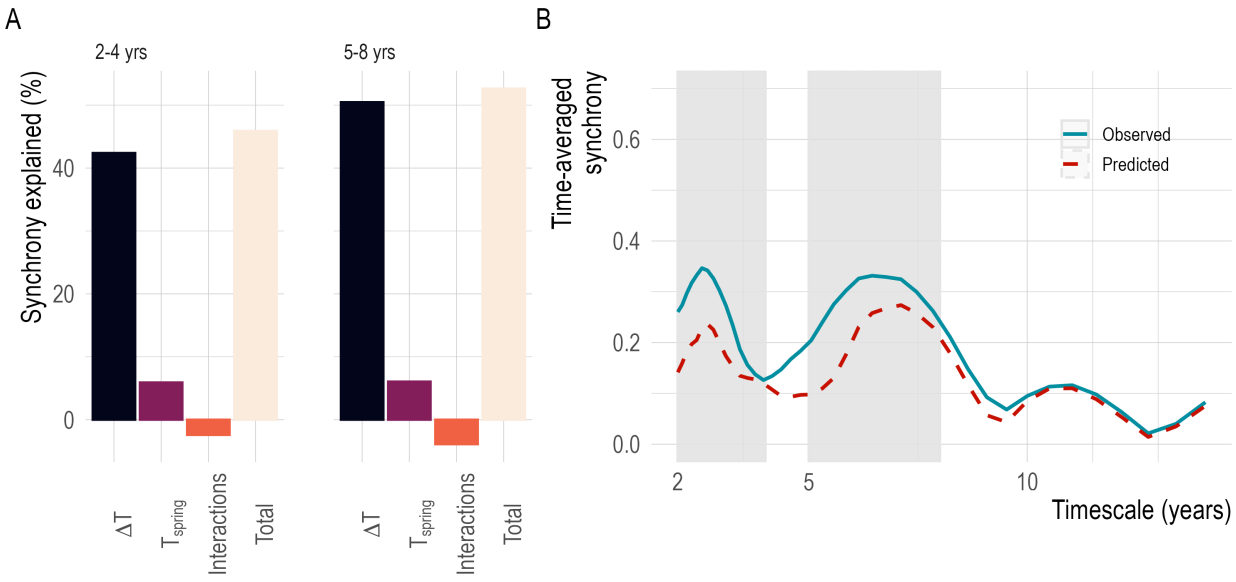

Figure 3: Spatial synchrony in community-wide masting is explained by the synchrony in summer temperature. (A) Fractions of synchrony in community-level masting explained by summer temperature cue (ΔT, see Methods), spring precipitation, and two-way interaction effects. Interaction effects can be positive (synergistic) or negative (antagonistic). B) The models explain substantial fractions of time-averaged spatial synchrony. The graph shows observed (solid blue line) and model-predicted (dashed red line) timescale-specific synchrony across all years, and compares these observations and model predictions across timescales. Grey bars highlight the two timescale bands (i.e., 2-4 and 5-8 years) for which the models at (A) were fitted. Cross terms exceed 10% at the 5–8-year band (Table 1), indicating violations of the wavelet Moran independence assumption and warranting caution in interpretation at this timescale.

Synchrony driven by summer temperatures. Community-wide synchrony at period of 2–4 was explained by summer temperature synchrony (Fig. 3, Table 1). Spring temperature effects were not significant, and interaction terms were weak, indicating that synchrony arises primarily via temperature-cued flowering initiation rather than joint effects with spring conditions. The quarter-cycle phase lags between masting and the summer temperature cue (Table 1) corresponds to seed production peaking about 1 year after high cue values, consistent with past observations and the interpretation that hot summers promote floral initiation for the following year (11; 20). The driver set explained a large share of the variance in timescale-specific synchrony, and model predictions matched observations across species and sites (2–4 y: 46.4% synchrony explained; Fig. 3). Contrary to expectation, NAO indices were not significant drivers of synchrony at the 5–8-year band (Table 1). In addition, the high proportion of cross terms for summer temperature (ΔT) at the long-period band (30%) suggests violations of the independence assumption underlying the wavelet Moran theorem, warranting caution in the interpretation of results at this temporal scale.

Within species, synchrony at both high- and low-frequency modes was associated with spatially coherent summer temperature (Table S1). Consequently, species-level synchrony driven by summer heat can aggregate into community-level mass flowering across the region due to largely shared masting cues. However, the consistently high cross terms at longer timescales indicate that the independence assumption of the wavelet Moran theorem is violated (11 - 16 ‰, Table S1), warranting caution in the interpretation of low-frequency effects. Accordingly, coherent summer temperature appears to be the dominant shared cue linking species and sites, although the drivers of low-frequency synchrony cannot be reliably distinguished given violations of model assumptions at longer timescales.

Shifting timescale structure of synchrony. The community-level short-period mode shortened after ~2005, shifting from a 3–4-year timescale toward ~2 years and weakening thereafter (Fig. 1). Long-period coherence (5–8 years) was higher before ~2010 and largely absent after ~2014 (Fig. 1), consistent with a recent loss of the low-period synchrony, though longer series are needed to separate a transient dip from a new state.

Within species, WMF indicates that amplitude is shared in some years but not others, and shows signals of temporal weakening of synchrony that is species- and period-dependent (Fig. 2). For example, in beech, long-period synchrony was largely absent, while the short-period synchrony declined over time (Fig. 2). In larch and oaks, the short-period synchrony also declined over time; while in spruce, the long-period synchrony declined (Fig. 2). In Scots pine (*Pinus sylvestris*), synchrony does not show a clear temporal trend, except for a strongly synchronized event in 2020 (Fig. 2). Thus, the attenuation of community-wide synchrony is not due to uniform declines within species; rather, our data suggest that species-specific changes in rhythms (period, phase) that increasingly fail to sum constructively, reducing community-level mass flowering that was evident in the early decades of the record. The recent fading of community-wide synchrony at both bands was also present in the independent dataset, lending additional support for the pattern (Fig. S2).

Discussion

We show that European temperate forests species exhibit regional, community-wide masting organized by two modes: a 2–4-year band and a secondary 5–8-year band. This reveals that community-level reproduction, previously thought unique to tropical Asian forests (5), is also a characteristic of European forest dynamics. The signal emerges from the dataset's broad spatial and temporal coverage, and from timescale-resolved wavelet metrics (WMF, WPMF) that separate short- and long-period components rather than pooling them (25; 1). The implications are broad: community-wide masting amplifies the ecosystem consequences of resource pulses by synchronizing peaks and troughs in seed supply across species and sites (2), with knock-on effects for seed consumers, tree recruitment, and ecosystem nutrient fluxes (33).

Community-wide synchrony that extends to the regional scale, as we show here, magnifies the ecosystem consequences of seed pulses. In high-seed years, trees reallocate carbon, reducing growth and defense while boosting pollination success and escape from predators via satiation (34; 35; 36). When seed production fluctuates in step across species and large spatial scales, these allocation shifts and their growth signatures are likely shared, which could produce coordinated swings in growth across the landscape. To the extent that is true, the longer period (5–8 years) synchrony band implies sub-decadal alternation between phases of improved landscape-scale tree growth (when reproduction is suppressed by weak cues) and phases of reduced growth during sustained reproduction; a hypothesis that can now be tested using the novel wavelet tools (25; 1). Joint reproduction also enhances predator satiation: generalist consumers that usually buffer shortfalls by switching foods can be overwhelmed when multiple species peak together, reducing per-capita predation across species (37). Thus, plant–seed consumer dynamics long associated with tropical systems may be more widespread, extending into temperate forests as well.

For consumers more generally, mast peaks generate resource pulses that drive primary consumer outbreaks that cascade through food webs (33), elevate risk of disease in animals and humans (38; 39), and increase allergenic pollen loads (40). Mast failures cause large-scale food scarcity, rodent population crashes (33), reproductive failure in insects, birds, and mammals (35), migration (41), and elevated human–wildlife conflict (42). When reproduction is synchronized

across species and across the landscape, these consequences are amplified: pulses in seed supply do not remain local but instead generate region-wide swings in consumer abundance, predation pressure, and disease dynamics. Short-period synchrony produces stronger, spatially extensive resource pulses than any single species can create, while long-period synchrony drives multi-year alternation between region-wide abundance and scarcity (6–8 y). A key next step is to test whether consumer communities exhibit corresponding multi-year cycling, though assembling spatially coherent, long-duration consumer data will be challenging.

Summer temperature emerged as the dominant correlate of masting synchrony, both within and across species, consistent with case studies reporting associations between masting and summer temperature and interpreting these relationships as enhanced floral initiation (11; 20). In contrast, spring temperature—although often an important local determinant of seed production (13)—did not contribute to regional synchrony. Interaction terms between drivers were generally weak, indicating that environmental influences did not combine synergistically or antagonistically to modify synchrony (1). Somewhat unexpectedly, the North Atlantic Oscillation was not a significant correlate of low-frequency synchrony. However, inference at longer timescales requires caution, as violations of model assumptions limit attribution of low-frequency structure to specific drivers. Moreover, Poland lies at the intersection of several large-scale teleconnection regimes (including the NAO, East Atlantic/Western Russia, and Scandinavian patterns), which may blur the imprint of any single mode.

The weakening of community-wide synchrony at both time bands indicates that, in recent years, temperate forests studied lost the large-scale coordination of reproduction that once generated multi-year pulses of resources; the disappearance of this pattern can be observed in Fig. 1B. Climate-related declines in regional masting have previously been documented in European beech, where summer temperatures act as the main cue for reproduction (30). As summers have warmed, cues have become increasingly frequent, causing reproduction to be triggered more often (31). Frequent flowering depletes stored resources (43), weakening plants' ability to respond to subsequent cues (31; 29); as a result, climate sensitivity and regional synchrony have both declined (30). This same pattern is reflected in our data, where the short-period component of synchrony in beech has changed structure and weakened over time. Similar

tendencies appear in other species, such as larch and oaks. In other species, such as spruce, only the long-period synchrony declined over time. These differences indicate that the loss of community-wide coordination arises not from uniform synchrony declines within species, but from a mix of species-specific shifts in synchrony and its timescale that no longer sum constructively at the community level. Variation in cue sensitivity is expected to determine how strongly each species' masting responds to ongoing climate change (8); because sensitivities differ among species (44; 19), responses will be non-uniform, and community-level general flowering is therefore the first to decline.

Apparent discrepancies with earlier analyses of the same dataset that used period-pooled correlation metrics and reported weak community-wide synchrony (21) reflect methodological rather than biological differences. Correlation-based approaches implicitly average across temporal frequencies and therefore cannot detect synchrony that is confined to specific timescale bands (1). When high- and low-frequency components differ in strength or phase, their effects can cancel when aggregated, yielding weak or absent net correlations despite strong band-limited synchrony (1). By contrast, timescale-explicit wavelet methods decompose synchrony by period and time, revealing community-wide reproductive alignment that is otherwise obscured by period-averaged analyses.

In closing, we show that temperate forests exhibit regional, community-wide masting at two timescales (2–4 and 5–8 y), with the short (2–4 y) band coordinated by spatially coherent summer temperatures, and that this coordination has weakened in recent decades. These findings extend the concept of general flowering beyond tropical forests. The recent decline in community synchrony—via species-specific shifts in synchrony and its timescale structure—implies smaller, less predictable resource pulses and a decoupling of consumer–resource dynamics at landscape scales. Building on this opens a new research program to test whether timescale-structured synchrony propagates through processes linked to masting, including forest recruitment (45), tree growth (43), disease risk (38), seed consumer dynamics (33), mycorrhizal abundance (46), and nutrient fluxes (47).

Materials and Methods

Masting data Seed-production data were obtained from the Polish State Forests and are based on annual seed harvests reported by local forest districts (30; 21). The dataset records the mass (kg) of seeds or cones collected per district per year and spans 1987–2022. It covers seven dominant forest-forming species: silver fir (*Abies alba*), European beech (*Fagus sylvatica*), European larch (*Larix decidua*), Norway spruce (*Picea abies*), Scots pine (*Pinus sylvestris*), sessile oak (*Quercus petraea*), and pedunculate oak (*Quercus robur*). These records document both the mass of seeds and cones collected (hereafter referred to as seeds for brevity) from seed stands in each district, and the demand driving collection intensity. Importantly, the synchrony in seed production is not driven by the demand (Fig. S4). Prior to 2008, oak harvests were not distinguished by species; therefore, records for the two oaks were summed for the entire time series. Synchrony of sessile and pedunculate oak for 2008–2022 (analysed separately and jointly) is shown in Fig. S5 and reveals strong temporal synchrony in seed production. Seeds are collected annually by contracted companies from assigned seed-collection stands, either from the ground or directly from tree canopies, depending on species. We compiled records from 432 forest districts (hereafter "sites"). For each species, we retained only sites with fewer than 80% zero records, yielding 238 sites for beech, 385 for oaks, 381 for pine, 79 for spruce, 93 for fir, and 138 for larch (Fig. 4). A high proportion of failure years (zero seed production) is a common feature of mast-seeding time series and was also present in our data (Fig. S6). However, re-analysis using an independent dataset (see below) with fewer zeroes (mean proportion of zeroes across species <5%) yielded qualitatively similar results, indicating that the prevalence of zeroes did not influence our conclusions.

Independent dataset used for replication

To independently test for community-wide "general flowering," we also analyzed the long-term dataset of the proportion of seed-producing trees (PST) compiled by the Polish State Forests for 16 Regional Forest Directorates. PST is the annual percentage of trees that fruited in a site (estimated to the nearest 10% and converted to proportions), providing a stand-level index of reproduction (48). These data were summarised at the level of Regional Forest Directorates and

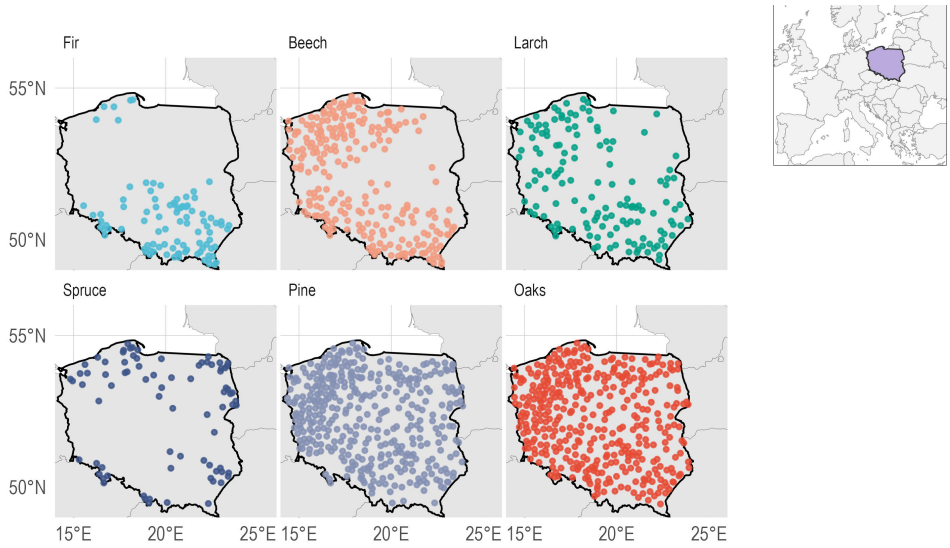

Figure 4: Study sites across Poland for silver fir (*Abies alba*), European beech (*Fagus sylvatica*), European larch (*Larix decidua*), Norway spruce (*Picea abies*), Scots pine (*Pinus sylvestris*), sessile oak (*Quercus petraea*), and pedunculate oak (*Quercus robur*); the oaks are pooled for the analysis as prior to 2008, oak harvests were not distinguished by species. The data were collected by the Polish State Forests and spans 1987–2022. Fig. S7 summarizes site-specific species co-occurance.

therefore represent reproduction at a regional (meta-population) scale. We used the data from 1987 - 2019 (data thereafter were unavailable) for the same set of species (*Abies alba*, *Fagus sylvatica*, *Larix decidua*, *Picea abies*, *Pinus sylvestris*, and *Quercus* spp.).

Weather data

Daily maximum temperature weather data for each site were obtained from the corresponding 0.1° grid cells of the E-OBS dataset ((49), v.31.0e). North Atlantic Oscillation indices were extracted from the National Oceanic and Atmospheric Administration.

Data analysis

Timescale-explicit synchrony. The *wsyn* package was used to analyze masting synchrony in R (50). We quantified timescale-specific spatial synchrony in seed production using the Wavelet Mean Field (WMF), which measures synchrony (in phase and amplitude) as a function of time and period across sites, and assesses statistical significance using the Wavelet Phasor Mean Field (WPMF). The WPMF measures synchrony in phase only, but provides a null model based on random phasors for inference (25; 2; 1). Each annual time series was normalised using a

Box–Cox transformation, detrended linearly, demeaned, and standardised to a variance of one (25). That step is recommended for wavelet coherence testing procedures described below, and includes detrending to remove trends that might otherwise obscure patterns of synchrony (25; 2; 1). Results were robust to alternative normalisation schemes, including analyses based on individually detrended, demeaned, and variance-standardised series, as well as the simplest approach relying only on demeaning each time series. Significance of WPMF was evaluated against 1,000 sets of random phasors, representing the null hypothesis of no synchrony except by chance (25).

WMF/WPMF were computed separately for each species (to characterize within-species regional synchrony) and then for all species' time series combined to test for community-level "general flowering." To assess temporal change in band-specific synchrony, we traced the WMF/WPMF fields through time, focusing on bands visible at the wavelet visualizations (~2–4y, ~5–8y). The methods and inference procedures follow recent applications (51; 2; 1). Independent replication of the community-level analyses was performed on the Regional Directorate flowering dataset (PST; 16 series; see "Independent dataset"), using the same procedures (Fig. S2, Fig. S3).

Driver attribution: coherence and multivariate modeling. To identify climatic drivers of synchrony, we computed *spatial wavelet coherence* between seed production and candidate variables on prespecified (based on visual assessment of the WMF) timescale bands. We tested summer (ΔT, see below) and spring temperature (mean in March and April) on both bands (2–4 y; 5–8 y), and North Atlantic Oscillation (NAO) indices (winter: Dec, Jan, Feb; summer: Jun, Jul, Aug) specifically for the 5–8 y band. Spring NAO was excluded due to high collinearity. We build separate models for weather cues and NAO indices.

Spatial wavelet coherence provides, for each band, a magnitude (association strength, p-value) and a phase (temporal offset), allowing estimation of cue–response lags (25; 1). We obtained the mean phase values (ϕ) for each band and driver by using the "fast" method introduced by (51), with 10,000 surrogate datasets (i.e., randomized datasets preserving spatiotemporal autocorrelation of input variables). Following established practice (2; 1), variables were advanced to *wavelet linear models* (WLMs), multivariate regressions in wavelet space used

to explain fractions of time-averaged synchrony and to partition contributions of predictors and their pairwise interactions (25; 26; 1). We assessed the significance of drivers by fitting a wavelet linear model to the selected drivers and by applying the wavelet Moran theorem (25; 26). We applied the *wavelet Moran theorem* and *synchrony attribution theorem* developed by (25) to (i) estimate the proportion of synchrony explained by WLMs and (ii) partition that explained synchrony among main effects and interactions (25; 26; 1). Following (25; 52), we then calculated cross-terms, a diagnostic of an independence assumption of the wavelet Moran theorem. Large cross-terms (>10%) indicate the assumption is unmet, with large cross-terms indicating that the unexplained synchrony in one location is correlated with the effect of the climate variable at other locations (25).

We used the summer ΔT as a masting cue across species. Generally, seed production in temperate tree species, including in our model species, is often triggered by subsequent cold (two years before seedfall, T2) and hot (one year before seedfall, T1) summers (10; 20). These two parameters (temperature in T1 and T2) can be collapsed into one by taking their difference (ΔT, i.e., the difference between mean maximum June, July temperatures in T1 and T2) (44). Thus, we used ΔT in our analysis as it allows the estimation of masting-cue relationships in with just one parameter (53). Inclusion of summer T1 and summer T2 temperatures separately would introduce collinearity into the model and bias estimates.

Acknowledgements

This study was funded by the European Union (ERC, ForestFuture, 101039066). JF was also supported by the Foundation for Polish Science (FNP). Views and opinions expressed are, however, those of the authors only and do not necessarily reflect those of the European Union or the European Research Council. Neither the European Union nor the granting authority can be held responsible for them. We would like to express our gratitude to the Directorate-General of State Forests for providing data on the abundance of seeds of major forest-forming species.

Author Contributions Statement

MB conceived the idea and designed the study, MB and VJ designed the analysis, VJ analyzed

the data, SJ, MKD, JF, and JS curated the data, and MB drafted the manuscript. All authors critically contributed to the data interpretation and revised the paper.

Declaration of interests

No competing interests to declare.

Data availability statement

The data and code supporting the results will be archived in the Open Science Framework (OSF).

References

[1] D. C. Reuman, *et al.*, *Ecology Letters* **28**, e70112 (2025).

[2] T. L. Anderson, L. W. Sheppard, J. A. Walter, R. E. Rolley, D. C. Reuman, *Ecology Letters* **24**, 337 (2020).

[3] D. J. Earn, S. A. Levin, P. Rohani, *Science* **290**, 1360 (2000).

[4] L. Egli, M. Schroter, C. Scherber, T. Tscharntke, R. Seppelt, *Nature* **588**, E7 (2020).

[5] S. Sakai, *Biological Journal of the Linnean Society* **75**, 233 (2002).

[6] M. Chechina, A. Hamann, *Journal of Tropical Ecology* **35**, 108 (2019).

[7] T. Qiu, *et al.*, *Nature Plants* **9**, 1044–1056 (2023).

[8] M. Bogdziewicz, *et al.*, *Trends in Ecology & Evolution* **39**, 851 (2024).

[9] I. S. Pearse, W. D. Koenig, D. Kelly, *New Phytologist* **212**, 546 (2016).

[10] G. Vacchiano, *et al.*, *New Phytologist* **215**, 595 (2017).

[11] V. Journé, *et al.*, *Nature Plants* **10**, 367 (2024).

[12] W. D. Koenig, J. M. Knops, W. J. Carmen, I. S. Pearse, *Ecology* **96**, 184 (2015).

[13] E. Fleurot, *et al.*, *Current Biology* **33**, 1117 (2023).

[14] J. M. LaMontagne, I. S. Pearse, D. F. Greene, W. D. Koenig, *Nature Plants* **6**, 460 (2020).

[15] M. Bogdziewicz, V. Journé, A. Hacket-Pain, J. Szymkowiak, *Ecology Letters* **26**, 754 (2023).

[16] S. J. Wright, O. Calderón, *Ecology Letters* **9**, 35 (2006).

[17] D. Ascoli, *et al.*, *Philosophical Transactions of the Royal Society B: Biological Sciences* **376**, 20200380 (2021).

[18] M. Shibata, T. Masaki, T. Yagihashi, T. Shimada, T. Saitoh, *Journal of Ecology* **108**, 1088 (2020).

[19] V. Journé, *et al.*, *Nature Communications* **16**, 9226 (2025).

[20] M. Hirsch, H. Puhlmann, H.-J. Klemmt, T. Seifert, *European Journal of Forest Research* **144**, 1505–1522 (2025).

[21] J. Szymkowiak, *et al.*, *PNAS* (2025).

[22] W. D. Koenig, J. M. H. Knops, *Ecology* **398**, 83 (2013).

[23] J. M. LaMontagne, *et al.*, *Ecology Letters* **27**, e14498 (2024).

[24] J. S. Clark, *et al.*, *Nature Communications 2021 12:1* **12**, 1 (2021).

[25] L. W. Sheppard, J. R. Bell, R. Harrington, D. C. Reuman, *Nature Climate Change* **6**, 610 (2016).

[26] L. W. Sheppard, E. J. Defriez, P. C. Reid, D. C. Reuman, *PLOS Computational Biology* **15**, e1006744 (2019).

[27] T. A. Shestakova, *et al.*, *PNAS* **113**, 662 (2016).

[28] B. B. Hansen, V. Grøtan, I. Herfindal, A. M. Lee, *Ecography* **43**, 1591 (2020).

[29] D. Kelly, J. Szymkowiak, A. Hacket-Pain, M. Bogdziewicz, *New Phytologist* **246**, 1975 (2025).

[30] J. Foest, *et al.*, *Ecology Letters* (2025).

[31] M. Bogdziewicz, *et al.*, *Global Change Biology* **27**, 1952 (2021).

[32] K. Kondrat, *et al.*, *EcoEvoRxiv* **https://doi.org/10.32942/X2H93H** (2025).

[33] R. S. Ostfeld, F. Keesing, *Trends in Ecology & Evolution* **15**, 232 (2000).

[34] D. Kelly, D. E. Hart, R. B. Allen, *Ecology* **82**, 117 (2001).

[35] J. D. Lauder, E. V. Moran, S. C. Hart, *Tree Physiology* **39**, 1071 (2019).

[36] R. Zwolak, P. Celebias, M. Bogdziewicz, *PNAS* **119**, e2105655119 (2022).

[37] L. M. Curran, C. O. Webb, *Ecological Monographs* **70**, 129 (2000).

[38] C. G. Jones, R. S. Ostfeld, M. P. Richard, E. M. Schauber, J. O. Wolff, *Science* **279**, 1023 (1998).

[39] B. A. Tonelli, C. Youngflesh, M. W. Tingley, *Proceedings of the National Academy of Sciences* **123**, e2511209123 (2026).

[40] Y. T. Tseng, S. Kawashima, S. Kobayashi, S. Takeuchi, K. Nakamura, *Science of the Total Environment* **698**, 134246 (2020).

[41] B. Zuckerberg, *et al.*, *Trends in Ecology & Evolution* **35**, 440 (2020).

[42] C. Tattoni, *et al.*, *Ecology and Evolution* **15**, e71693 (2025).

[43] A. Hacket-Pain, *et al.*, *PNAS* **122**, e2423181122 (2025).

[44] D. Kelly, *et al.*, *Ecology Letters* **16**, 90 (2013).

[45] M. Bogdziewicz, *et al.*, *Ecology letters* **27**, e14514 (2024).

[46] T. J. Michaud, I. S. Pearse, H. Kauserud, C. J. Andrew, P. G. Kennedy, *Ecology Letters* p. e14460.

[47] H. Müller-Haubold, D. Hertel, C. Leuschner, *Ecosystems* **18**, 1083 (2015).

[48] M. B. Pesendorfer, *et al.*, *Global Change Biology* **26**, 1654 (2020).

[49] R. C. Cornes, G. van der Schrier, E. J. van den Besselaar, P. D. Jones, *Journal of Geophysical Research: Atmospheres* **123**, 9391 (2018).

[50] D. C. Reuman, T. L. Anderson, J. A. Walter, L. Zhao, L. W. Sheppard, *wsyn: Wavelet Approaches to Studies of Synchrony in Ecology and Other Fields* (2021). R package version 1.0.4.

[51] L. W. Sheppard, P. C. Reid, D. C. Reuman, *EPJ Nonlinear Biomedical Physics* **5**, 1 (2017).

[52] C. A. Rodenberg, J. A. Walter, K. J. Haynes, *Ecology Letters* **28**, e70140 (2025).

[53] J. Szymkowiak, *et al.*, *Ecology Letters* **27**, e14474 (2024).

Supporting Information

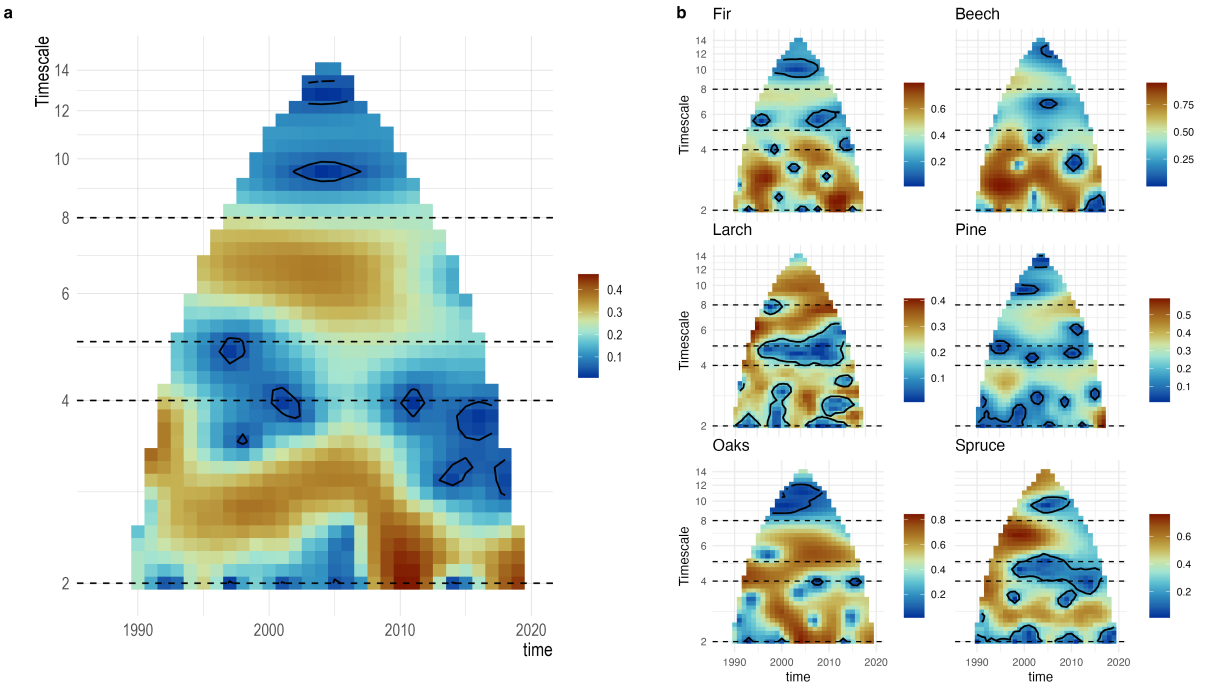

Figure S1: Wavelet phasor mean field (WPMF) magnitude plots of time- and timescale-specific spatial synchrony in seed production for all studied species (a) and for each species separately (b). Black contours indicate statistically significant synchrony. At (a) all time series from all species were analysed jointly and therefore reflect the combined effects of within- and among-species synchrony, i.e., community-level synchrony. Species-specific (within-species) synchrony is shown in (b). The analysis is based on seed production data collected between 1987 and 2022 across 432 sites in temperate Europe. Species include silver fir (*Abies alba*), European beech (*Fagus sylvatica*), European larch (*Larix decidua*), Norway spruce (*Picea abies*), Scots pine (*Pinus sylvestris*), sessile oak (*Quercus petraea*), and pedunculate oak (*Quercus robur*). Prior to 2008, oak harvests were not distinguished by species; therefore, records for the two oaks were pooled for the entire time series. Results based on an independent dataset that replicated the pattern are provided in Fig. S2.

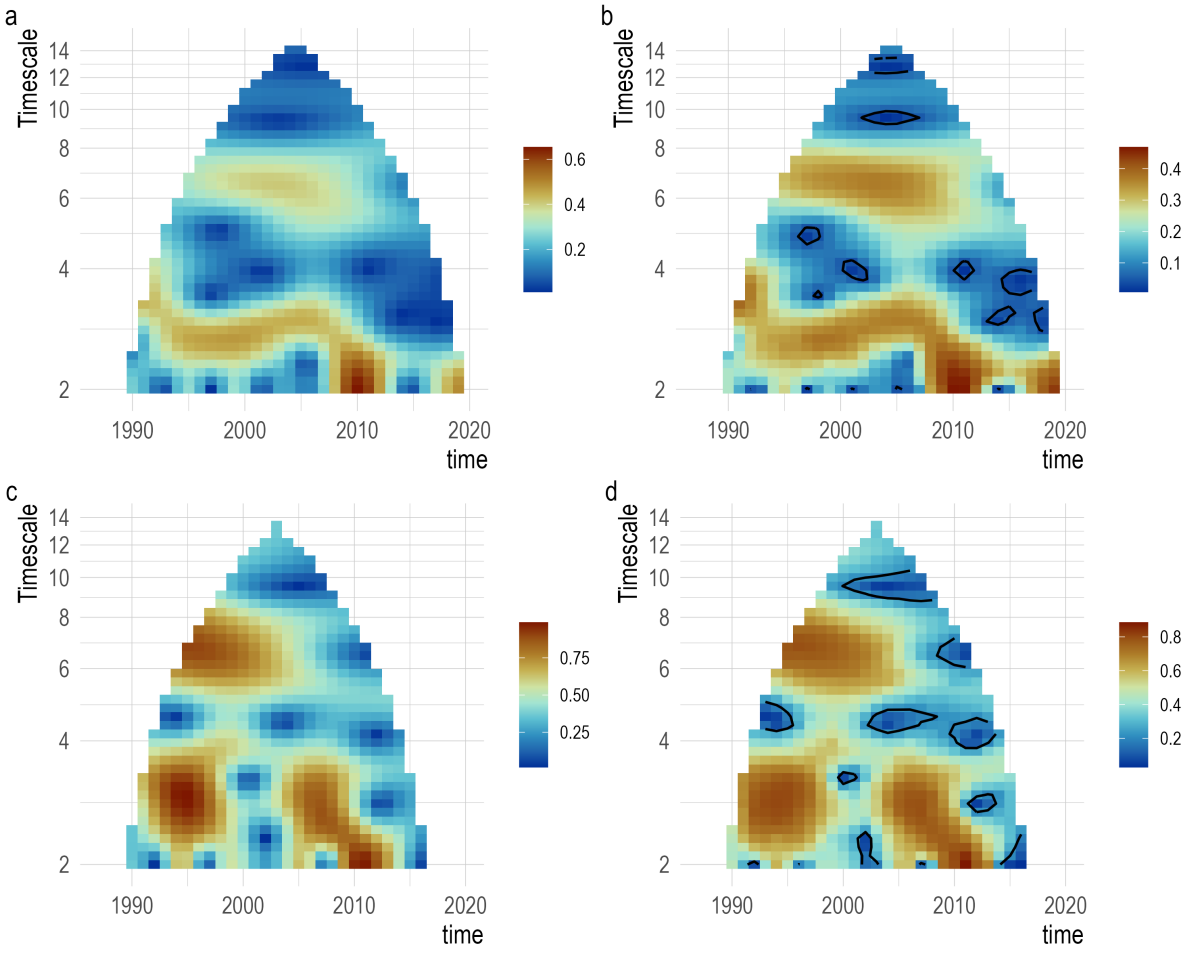

Figure S2: Independent dataset replicates the dual-band synchrony that organizes community-wide masting in temperate forests. The top panels show the analysis as reported in the main text (432 sites, and 1314 site-species combinations), while the bottom panel shows an independent dataset from the same region (16 sites, 151 site-species combinations). Left column (a, c) shows wavelet mean field (WMF), while the right column shows wavelet phasor mean field (WPMF) magnitude plots (b, d). In this analysis, time series from all species were analysed jointly and therefore reflect the combined effects of within- and among-species synchrony, i.e., community-level synchrony.

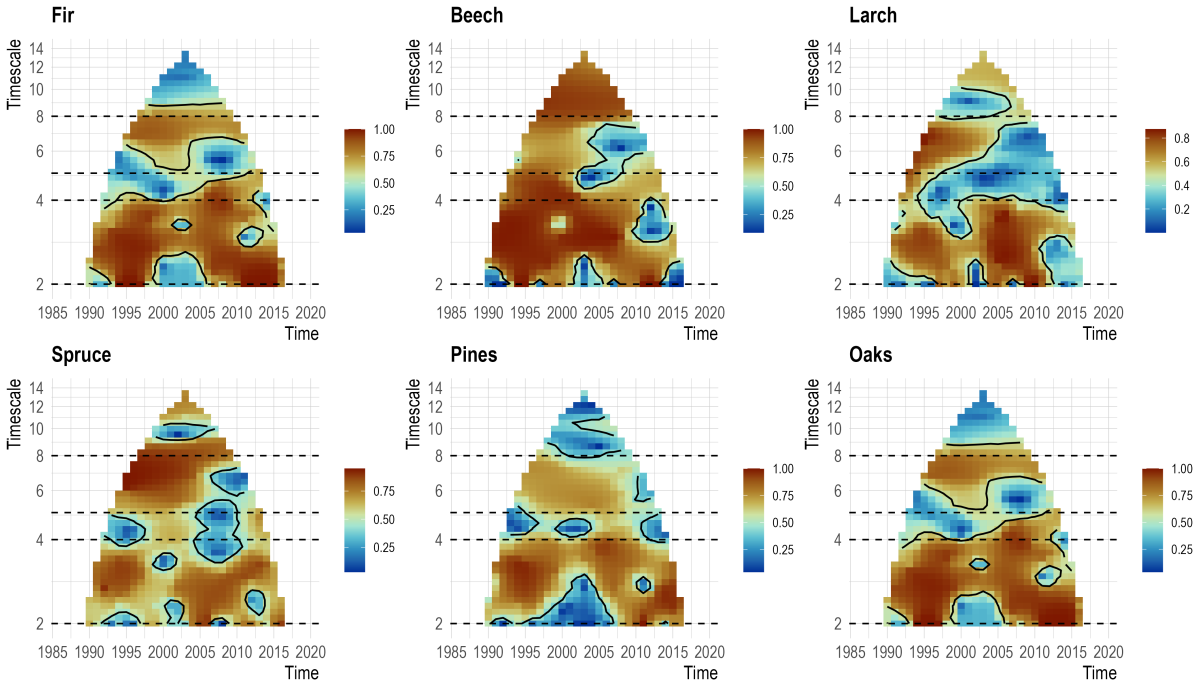

Figure S3: Dual-band interspecific synchrony that underlies community-wide masting in temperate forests (independent dataset). Wavelet mean field (WMF) magnitude plots of time- and timescale-specific spatial synchrony in seed production for each species separately. Black contours indicate statistically significant synchrony as determined from the wavelet phasor mean field (WPMF), with the WPMF plots in Fig. S1. The analysis is based on seed production data collected between 1987 and 2019 across 16 sites in temperate Europe. Species include silver fir (*Abies alba*), European beech (*Fagus sylvatica*), European larch (*Larix decidua*), Norway spruce (*Picea abies*), Scots pine (*Pinus sylvestris*), sessile oak (*Quercus petraea*), and pedunculate oak (*Quercus robur*).

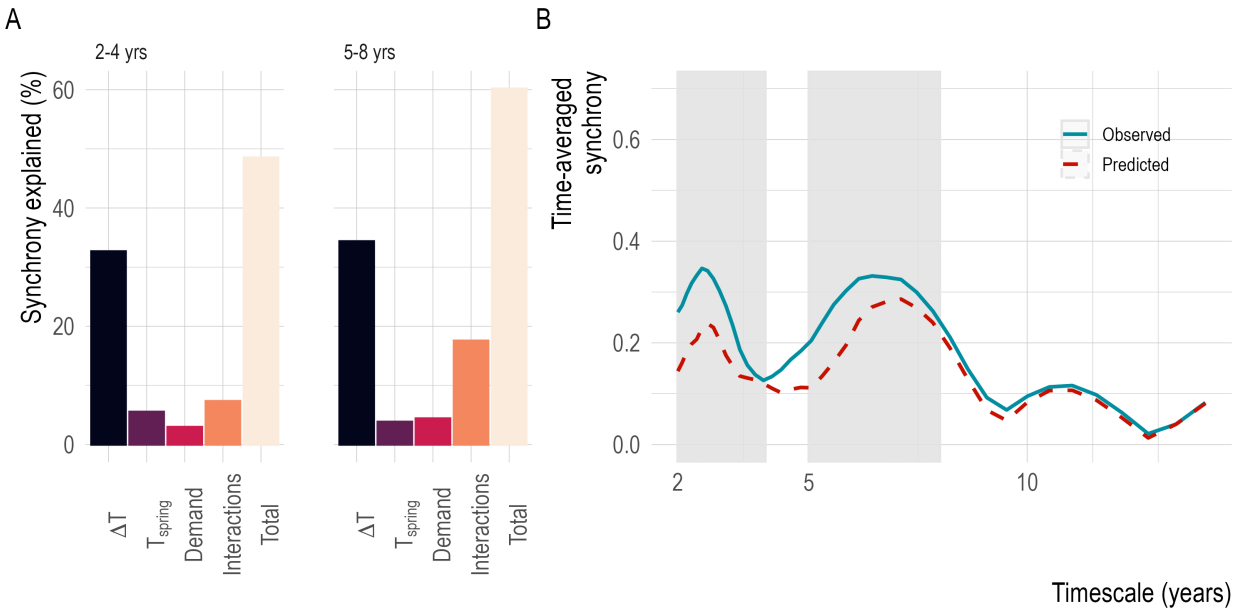

Figure S4: Spatial synchrony in community-wide masting is explained by the synchrony in summer temperature. (A) Fractions of synchrony in community-level masting explained by summer temperature cue (ΔT, see Methods), spring precipitation, Demand, and three-way interaction effects. Interaction effects can be positive (synergistic) or negative (antagonistic). B) The models explain substantial fractions of time-averaged spatial synchrony. The graph shows observed (solid blue line) and model-predicted (dashed red line) timescale-specific synchrony across all years, and compares these observations and model predictions across timescales. Grey bars highlight the two timescale bands for which the models at (A) were fitted.

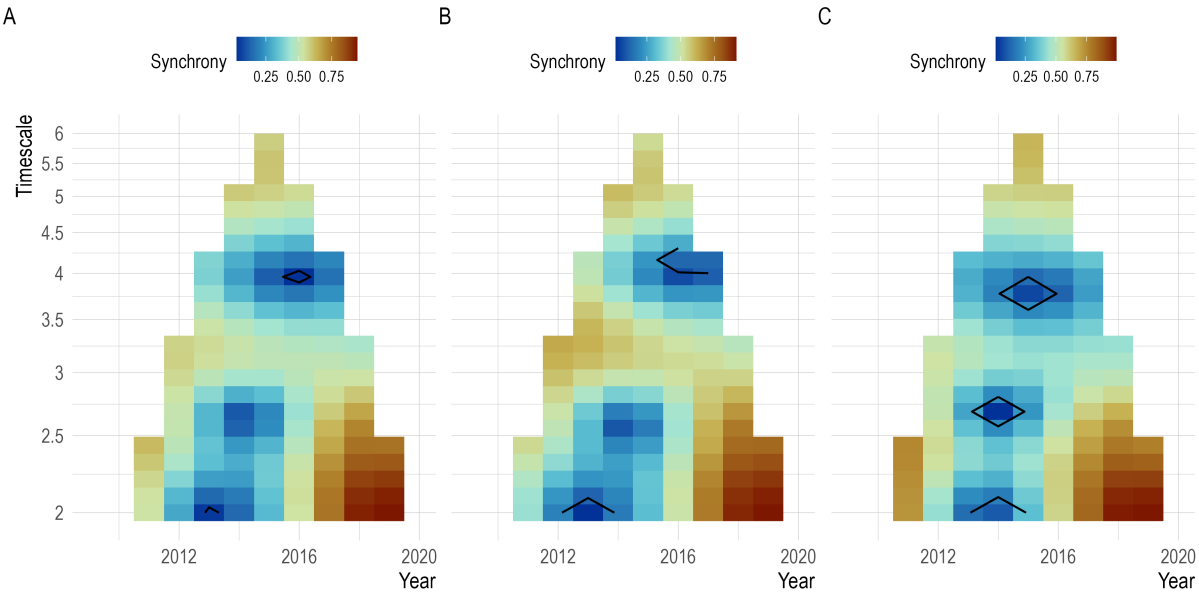

Figure S5: High within and among-species synchrony in oaks, for the period when records allow separation of the two species (in 2008-2022). Wavelet mean field (WMF) magnitude plots of time- and timescale-specific spatial synchrony in seed production for A) pedunculate and sessile oak analyzed together (N=538 sites); B) pedunculate oaks (N=330 sites) and C) Sessile oaks separately (N=208 sites). Black contours indicate statistically significant synchrony as determined from the wavelet phasor mean field (WPMF).

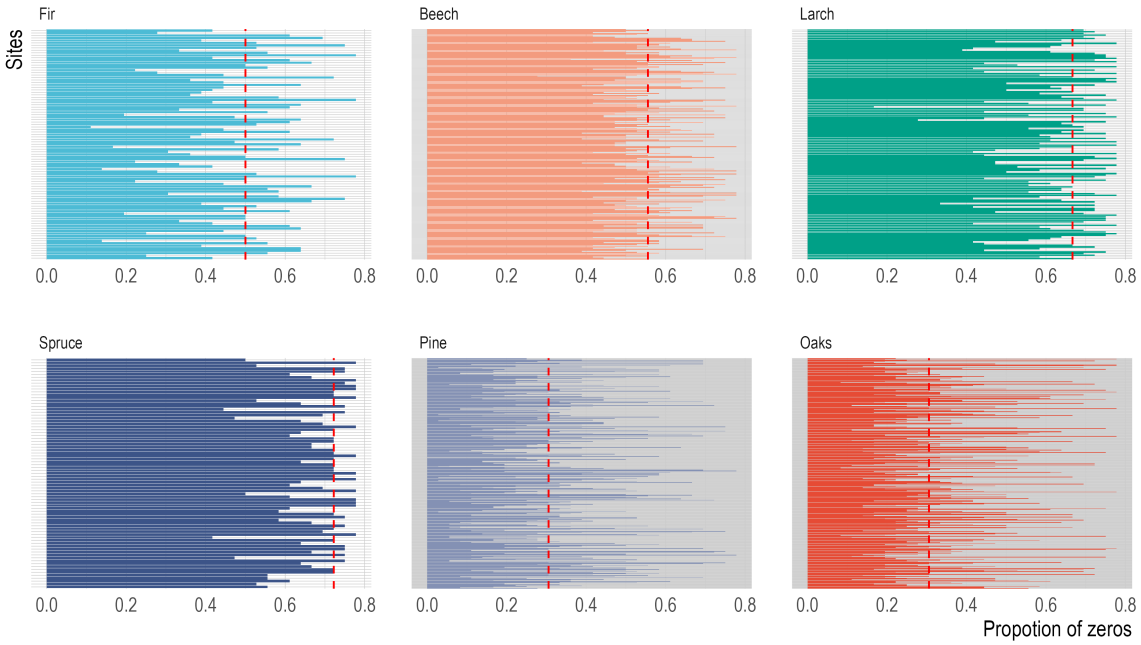

Figure S6: Proportion of zero records within each taxa time series. The red dotted vertical line represent median value; Beech, 0.56; Fir, 0.50; Larch, 0.67; Oaks, 0.31; Pine, 0.31; Spruce, 0.72.

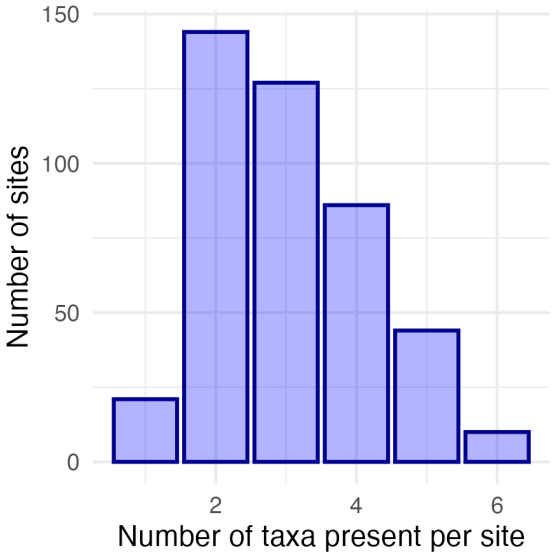

Figure S7: Species co-occurrence across sites. Bars show the number of taxa present per site (1–6) in the analyzed dataset (N=432 sites). Oaks are pooled together (see Methods).

Table S1: Species-specific relationship between masting synchrony and driver variables. P-values are from tests of spatial wavelet coherence. Phase relationships (ϕ) for drivers were obtained from multi-predictor wavelet linear models. Phase relationships are given in fractions of π, for significant drivers. Negative phase relationships that are not approximately in-phase ($\phi \approx 0$, interpreted as $-0.25 < \phi < 0.25$) or anti-phase ($\phi \approx \pm 1$, interpreted as $\phi < -0.75$ or $\phi > 0.75$) indicate that masting lags the driver variable; positive phase relationships that are not approximately in-phase or anti-phase indicate that mast peaks precede those of the driver variable. Cross term is a diagnostic of the wavelet Moran theorem; no values were reported for NAO indices because those climate indices are not spatially resolved.

Variable	Species	Timescale	p-value	Mean phase	Cross term
ΔT	*Abies alba*	2-4	0.02	-1.45	7.38
		5-8	0.02	-0.56	16.1
	Fagus sylvatica	2-4	0.0009	-0.36	4.37
		5-8	0.003	-0.036	13.4
	Larix decidua	2-4	0.08	0.70	5.04
		5-8	0.41	-	16.5
	Picea abies	2-4	0.01	0.32	10.1
		5-8	0.01	-0.46	25.9
	Pinus sylvestris	2-4	0.18	-	5.04
		5-8	0.004	-0.95	16.5
	Quercus spp.	2-4	0.64	-	11.4
		5-8	0.02	-0.60	26.6
T_{spring}	*Abies alba*	2-4	0.13	-	7.38
		5-8	0.31	-	16.1
	Fagus sylvatica	2-4	0.57	-	4.37
		5-8	0.30	-	13.4
	Larix decidua	2-4	0.13	-	5.04
		5-8	0.83	-	16.5
	Picea abies	2-4	0.33	-	10.1
		5-8	0.12	-	25.9
	Pinus sylvestris	2-4	0.18	-	5.04
		5-8	0.89	-	16.5
	Quercus spp.	2-4	0.76	-	11.4
		5-8	0.96	-	26.6
NAO_{winter}	*Abies alba*	5-8	0.15	-	-
	Fagus sylvatica	5-8	0.52	-	-
	Larix decidua	5-8	0.02	-0.28	-
	Picea abies	5-8	0.05	-0.62	-
	Pinus sylvestris	5-8	0.23	-	-
	Quercus spp.	5-8	0.28	-	-
$NAO_{summerT1}$	*Abies alba*	5-8	0.35	-	-
	Fagus sylvatica	5-8	0.21	-	-
	Larix decidua	5-8	0.17	-	-
	Picea abies	5-8	0.34	-	-
	Pinus sylvestris	5-8	0.80	-	-
	Quercus spp.	5-8	0.52	-	-